

# Modeling of triple concave friction pendulum bearings for seismic isolation of buildings

Muhammet Yurdakul<sup>1a</sup> and Sevket Ates<sup>\*2</sup>

<sup>1</sup>Department of Civil Engineering, Bayburt University, Bayburt, Turkey

<sup>2</sup>Department of Civil Engineering, Karadeniz Technical University, Trabzon, Turkey

(Received July 11, 2010, Revised March 31, 2011, Accepted August 17, 2011)

**Abstract.** Seismic isolated building structures are examined in this study. The triple concave friction pendulum (TCFP) is used as a seismic isolation system which is easy to be manufactured and enduring more than traditional seismic isolation systems. In the TCFP, take advantage of weight which pendulum carrying and it's geometry in order to obtain desirable result of seismic isolation systems. These systems offer advantage to buildings which subject to severe earthquake. This is result of damping force of earthquake by means of their internal constructions, which consists of multiple surfaces. As the combinations of surfaces upon which sliding is occurring change, the stiffness and effective friction change accordingly. Additionally, the mentioned the TCFP is modeled as of a series arrangement of the three single concave friction pendulum (SCFP) bearings. A two dimensional- and eight- story of a building with and without isolation system are used in the time history analysis in order to investigate of the effectiveness of the seismic isolation systems on the buildings. Results are compared with each other to emphasize efficiency of the TCFP as a seismic isolation device against the other friction type isolation system like single and double concave surfaces. The values of the acceleration, floor displacement and isolator displacement obtained from the results by using different types of the isolation bearings are compared each other. As a result, the findings show that the TCFP bearings are more effective devices for isolation of the buildings against severe earthquakes.

**Keywords:** seismic isolation; single concave friction pendulum; double concave friction pendulum; triple concave friction pendulum; severe earthquake

---

## 1. Introduction

Seismic isolation systems generally make structure more resistant to earthquake ground motions. This is because of the positive effects; the seismic isolation techniques have been rapidly a widespread application. Most of the seismic isolation systems currently in use provide friction properties as their energy dissipation mechanism. Theoretical and experimental research studies (Mostaghel and Tanbakuchi 1983, Lin and Tadjbakhsh 1986, Kelly 1999, Tsai *et al.* 2003, Morgan and Mahin 2008, Panchal *et al.* 2010, Khoshnoudian and Rabiei 2010) have immensely investigated frictional and rubber based seismic isolation systems. Zayas (1986) introduced one of the most

---

\*Corresponding author, Ph.D., E-mail: [sates@ktu.edu.tr](mailto:sates@ktu.edu.tr)

<sup>a</sup>E-mail: [myurdakul@bayburt.edu.tr](mailto:myurdakul@bayburt.edu.tr)

effective isolation systems, namely single concave friction pendulum (SCFP) bearing offer developments in strength, life span, resistance of severe earthquake and easy to installation. That is why, many of studies regarding earthquake-resistant structures have been focused on developing more versatile and economic isolation systems such as friction pendulum. Hence double concave friction pendulum (DCFP) and triple concave friction pendulum (TCFP) have been come up with. The DCFP consists of two spherical stainless steel surfaces and an articulated slider covered by a Teflon-based high bearing capacity composite material. On the other hand, the TCFP is also consisted of two facing concave stainless steel surfaces, but an articulated slider is separately placed between the two spherical stainless steel surfaces. Namely, in the later system motions occur in three sliding surfaces. So the system is named as triple. The TCFP exhibits multiple changes in stiffness and damping properties during its motion. It is provided increasing amplitude of displacement. The great advantage of the TCFP bearing is that there is motion on two inner concave surfaces in small amplitude of earthquake while there is no motion on outermost surfaces. However, the motion occurs on the outermost surfaces in case of more severe earthquake. Owing to the fundamental law of the TCFP, chafing does not occur on these surfaces and the system provides long living usage of these devices than the SCFP and the DCFP bearings. Numerical investigations have been carried out on the base isolation effect of the DCFP bearings by Kim and Yun (2007). Nonlinear time history analyses have been carried out on a simplified bridge model to examine the complex behavior of the DCFP and bridge under various earthquake inputs with different intensities, as well. Especially, benefits of the tri-linear DCFP over the bi-linear DCFP are investigated.

Development of the friction type seismic isolation systems has still been progressed. The theoretical force-displacement relationship was verified by Fenz and Constantinou (2006) through characterization testing of bearings with sliding surfaces having the same and different radii of curvature and coefficients of friction. The variable friction pendulum system (VFPS) was developed by Panchal and Jangid (2008). Soni *et al.* (2010) presented the behavior of asymmetric building isolated by the double variable frequency pendulum isolator (DVFPI). The DVFPI is an adoption of single variable frequency pendulum isolator (VFPI). It was found that the performance of the DVFPI can be optimized by designing the top sliding surface initially softer and smoother relative to the bottom one.

The principles of operation and force-displacement relationships of the TCFP, the modified SCFP, and the DCFP with sliding surfaces of different displacement capacities are developed by Fenz and Constantinou (2008a, b). In these studies, it has been shown that when properly configured, these bearings provide stiffness and damping that change desirably with increasing displacement. Fenz and Constantinou (2008c) proposed series model composed of existing nonlinear elements in order to be modeled the TCFP bearing by assembling the SCFP and the gap elements in SAP2000 (1997). However, the behavior of the TCFP bearing is not exactly that of a series arrangement of the SCFP bearing. So, the authors described how to modify the input parameters of the series model in order to accurately retrace real force-displacement behavior exhibited by the TCFP. Fenz and Constantinou (2008d) verified the principles of operation and force-displacement relationships of a class of multi-spherical sliding bearings that exhibit adaptive behavior. The new base isolator called the multiple trench friction pendulum system (MTFPS) is proposed by Tsai and Lin (2009), and Tsai *et al.* (2010). The proposed MTFPS isolator is composed of a trench concave surface and several intermediate sliding plates in two orthogonal directions. Mathematical formulations have been also derived to examine the characteristics of the

proposed MTFPS isolator possessing multiple intermediate sliding plates. Fadi and Constantinou (2010) reported that development of tools of simplified analysis and demonstration of their accuracy is required for the new developed TCFP bearings. So, these tools are described and validation studies based on a large number of nonlinear response history analysis results are presented in the paper. It is shown that simplified methods of analysis systematically provide good and often conservative estimates of isolator displacement demands and good estimates of isolator peak velocities. The performance-based seismic design of the Sabiha Gokcen International Airport Terminal Building in Istanbul, Turkey utilizing seismic-isolation concept with the TCFP bearings is achieved (Zekioglu *et al.* 2009).

The aim of this paper is to implement the series model proposed by Fenz and Constantinou (2008c) on a two dimensional and eight story-building when the structure is subjected to the three different earthquake ground motions. The motions are the GBZ000 component of the 17 August 1999 Kocaeli Earthquake recorded at Gebze station, the TCU129-W component of the 1999 Chi-Chi earthquake recorded at TCU129 station and the ELC-270 component of the 1940 Imperial Valley earthquake recorded at 117 El-Centro Array #9 station available from PEER database are used as earthquake records in the time history analysis. Additionally the SCFP and the DCFP bearings are also used for comparing purpose. On account of the fact that the bearing model recently has been developed, its computer application and its behavior have not been well known. This study will serve to the researchers and engineers in field of the earthquake engineering in order to apperceive the concept of the TCFP bearings for seismically isolated buildings and other structures.

## 2. Principles of the TCFP bearings

The TCFP bearing shown in Fig. 1 is consisted of two facing concave stainless steel surfaces coated with Teflon separated by a placed slider assembly.  $R_i$  is the radius of curvature of surface  $i$ ,  $h_i$  is the radial distance between the pivot point and surface  $i$  and  $\mu_i$  is the coefficient of friction at the sliding surface  $i$ ,  $d_i$  is the displacement capacity of the surface  $i$ . Outer concave plates have effective radii  $R_{eff1} = R_1 - h_1$  and  $R_{eff4} = R_4 - h_4$ . The articulated slider assembly consists of two concave plates separated by a rigid slider. Though the innermost slider is rigid, the assembly as a whole has the capability to rotate to accommodate differential rotations of the top and bottom plates. The friction coefficients on these concave plates are  $\mu_1$  and  $\mu_4$ . The inner concave plates have effective radii  $R_{eff2} = R_2 - h_2$  and  $R_{eff3} = R_3 - h_3$ . Additionally, these surfaces are also coated with Teflon. The friction coefficients on these concave plates are  $\mu_2$  and  $\mu_3$ . This leads to motion of slider between up and down stainless of steel surfaces of slide plates. Unlike the SCFP and DCFP, in the TCFP bearing there is no mechanical constraint defining which defined location of pivot point (Fenz and Constantinou 2008a, b).

Instead of this, pivot point corresponds to immediate center of zero velocity of slider assembly. This center is not a fixed point. It changes during sliding on the concave surfaces. Although, because the immediate center of zero velocity of up and down parts of the slider are always opposite directions, the immediate center of velocity must always be between of them. In generally, the slider height is small than radii of curvature and there is little error occurred by assuming the immediate center of velocity is fixed at middle of height of the articulated slider assembly. Like to the DCFP and the TCFP bearings enable to simultaneously sliding on multiple concave plates.

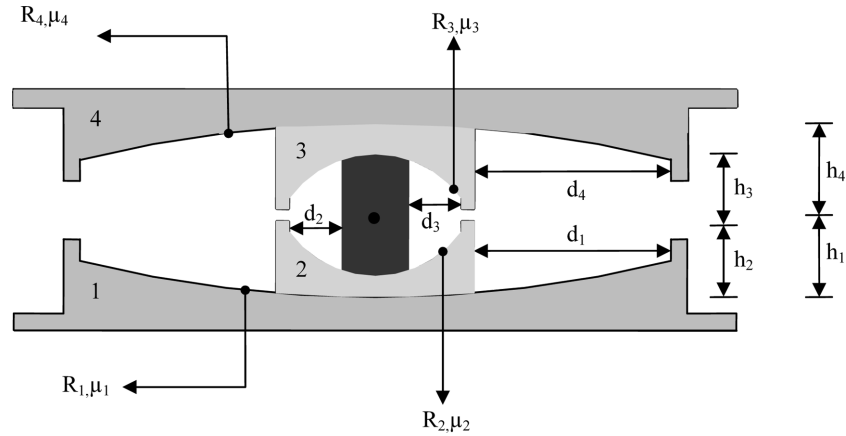


Fig. 1 The cross-section of the TCFP bearing and its definition of dimensions

Hence it is constructed smaller than the SCFP bearing using the same general displacement capacity. In case economic benefits are taken into account, there is insignificant differentiation in the cost of the SCFP and the DCFP bearings of size. However, the TCFP bearing is cost effective as per bearing size and displacement capacity.

**3. Series model of the TCFP bearing**

There are practicable no hysteresis rules or nonlinear elements present in structural program that can be used triple friction model in series model for response history analysis. Series model consist of linear element which can be used in present software structural analysis program. But, the TCFP bearing is not exactly like a model organized as a three SCFP bearing in series model although it is similar. Series models are favored because of their implementation in available commercial structural analysis program such as SAP2000 (2007). It has nonlinear elements modeling rigid linear behavior of the SCFP bearings. However, one behavioral event is preventing correctly modeling the TCFP bearing as a three SCFP bearing. This event is there is no sliding simultaneous on spherical concave surfaces 1 and 2. This observation is experimentally and analytically achieved by Fenz and Constantinou (2008c). At first, sliding occurs on spherical innermost concave surfaces 2 and 3 then stops when sliding starts on outermost spherical concave surfaces 1 and 4. Then sliding starts on innermost surfaces 2 and 3 again when the outer concave plates contacts restrainer displacement. The mentioned possible motions are depicted in Fig. 2.

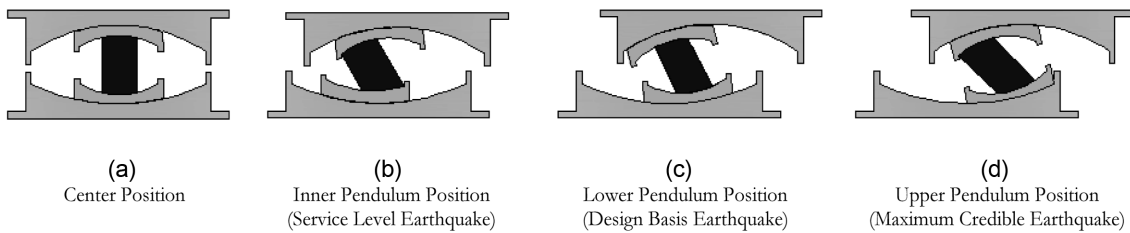


Fig. 2 The possible positions of the TCFP bearing

Schematic of three SCFP bearing elements connected in series is shown in Fig. 3. In this figure,  $1/\bar{R}_{effi}$ ,  $\bar{\mu}_i$  and  $\bar{d}_i$  represent the stiffness of the spring based on the effective radius of curvature  $i$ ; the velocity dependent coefficient of friction and the displacement of the gap link element, respectively. Overbar notation is employed to symbolize parameters and responses related with the series model. In the other hand, normal notation is employed to symbolize parameters and responses related with the TCFP bearing.

In the series model, displacement of element  $i$  begins when horizontal force,  $F$ , exceeds the friction force. The friction force for each concave surface by means of  $\bar{F}_{fi} = \bar{\mu}_i W$  where  $W$  is the vertical load acting on the bearing. Motion of  $i$  elements stop when  $i_{th}$  element displacement becomes equal to displacement capacity  $\bar{d}_i$ . This occurs at an applied horizontal force of

$$F_i = \frac{W}{\bar{R}_{effi}} \bar{d}_i + \bar{\mu}_i W \tag{1}$$

The force-displacement relationship can be obtained by considering the series model is depicted in Fig. 4. The model nearly gives the same actual force-displacement relationship which exhibits the

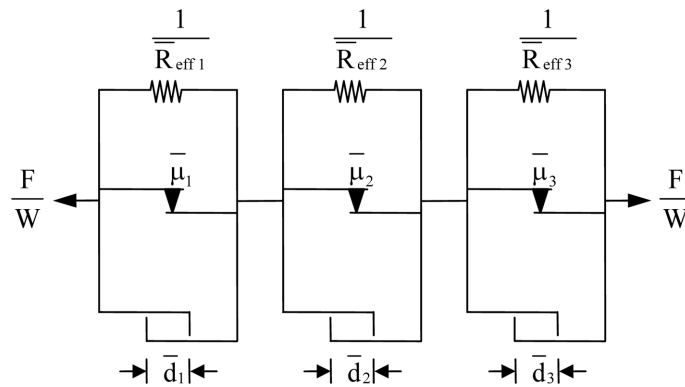


Fig. 3 The three SCFP elements in series model representing the TCFP bearing

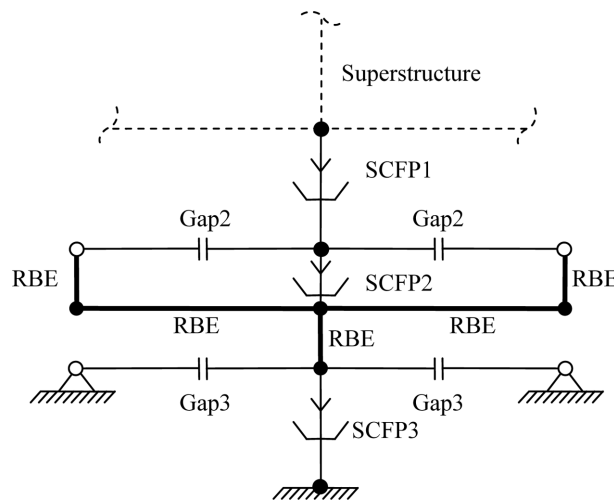


Fig. 4 Series model of the TCFP bearing used in SAP2000

TCFP bearing. The series model is recommended by Fenz and Constantinou (2008c). Fig. 4 shows how to create the series model of the TCFP bearing in SAP2000 is by assembling of three friction pendulum (SCFP) link elements, four gap link elements, and five rigid beam elements (RBE).

#### 4. Formulation of the series model of the TCFP

In the series modeling scheme proposed by Fenz and Constantinou (2008c), the SCFP1 link element represents the combined behavior of inner surfaces 2 and 3, the SCFP2 link element represents the behavior of outer surface 1 and the SCFP3 link represents outer surface 4. Since there is no adjustment made to the vertical load supported by the bearings, to ensure that sliding initiates correctly for each element there are no modifications made to the coefficients of friction. That is

$$\bar{\mu}_1 = \mu_2 = \mu_3 \quad (2)$$

$$\bar{\mu}_2 = \mu_1 \quad (3)$$

$$\bar{\mu}_3 = \mu_4 \quad (4)$$

The actual behavior is sliding occurring only on surfaces 2 and 3. In the series model, sliding takes place only for SCFP1 link element. And so, it is essential that

$$\bar{R}_{eff\ 1} = R_{eff\ 2} + R_{eff\ 3} \quad (5)$$

The effective radius of the SCFP2 link element in the series model is obtained by equating the stiffness given by the series model with the actual stiffness exhibited by the bearing

$$\frac{W}{\bar{R}_{eff\ 1} + \bar{R}_{eff\ 2}} = \frac{W}{R_{eff\ 1} + R_{eff\ 3}} \quad (6)$$

and combining Eqs. (5) and (6), the effective radius for the SCFP2 link element can be obtained as

$$\bar{R}_{eff\ 2} = R_{eff\ 1} - R_{eff\ 2} \quad (7)$$

In a similar way, the effective radius of the SCFP3 link element in the series model is attained by equating the stiffness given by the series model with the actual stiffness exhibited by the bearing

$$\frac{W}{\bar{R}_{eff\ 1} + \bar{R}_{eff\ 2} + \bar{R}_{eff\ 3}} = \frac{W}{R_{eff\ 1} + R_{eff\ 4}} \quad (8)$$

by combining Eqs. (5), (7) and (8), the effective radius for the SCFP3 link element can be obtained as

$$\bar{R}_{eff\ 3} = R_{eff\ 4} - R_{eff\ 3} \quad (9)$$

In the series model, gap link elements are also used in order to achieve the true force-displacement relationship of the TCFP bearing. So, displacements at which the gap link element are given by following equations

$$\bar{d}_2 = \frac{R_{eff\ 1} - R_{eff\ 2}}{R_{eff\ 1}} d_1 \quad (10)$$

$$\bar{d}_3 = \frac{R_{eff\ 4} - R_{eff\ 3}}{R_{eff\ 4}} d_4 \quad (11)$$

If desired to model the total displacement capacity of the bearing, the displacement capacity of the SCFP1 link element can be assigned as

$$\bar{d}_1 = (d_1 + d_2 + d_3 + d_4) - (\bar{d}_2 + \bar{d}_3) \quad (12)$$

The rate parameter,  $a$ , is adjusted to properly model the velocity dependence of the coefficient of friction on outer surfaces 1 and 4. This is provided by indicating

$$\bar{a}_2 = \frac{R_{eff\ 1}}{R_{eff\ 1} - R_{eff\ 2}} a_1 \quad (13)$$

$$\bar{a}_3 = \frac{R_{eff\ 4}}{R_{eff\ 4} - R_{eff\ 3}} a_4 \quad (14)$$

For the SCFP1 link element of the series model, the rate parameter can be specified as half of the average of the rate parameters on surfaces 2 and 3 of the TCFP bearing. Therefore

$$\bar{a}_1 = \frac{a_2 + a_3}{4} \quad (15)$$

## 5. Numerical computations

Nonlinear time history analysis of the isolated and non-isolated reinforced concrete building structure is performed. A two dimensional- and eight story-building structure is selected as an analytical model in order to execute the analysis. The TCFP bearings are to be opted for the isolation devices and placed between the bottom of the columns and the foundation. The TCFP bearings are modeled as the series model of the TCFP bearing in SAP2000 (2007) by assembling of three single concave friction pendulum (SCFP) link elements, four gap link elements and five rigid beam elements (RBE). A schematic model of the structure mentioned above is shown in Fig. 5. The cross sectional properties of the column and beam elements of the structure are given in Table 1. Damping ratio is specified as 5%. Effective radius of curvature, frictional properties and displacement capacities of the TCFP bearings are given in Table 2.

Input parameters in series model, which are calculated by using values of Table 1 and Eqs. (5) to (15), are given in Table 3 in which SCFP1 link element represents inner surfaces 2 and 3, SCFP2 link element represents outer surface 1, and SCFP3 link element represents outer surface 4. Sum of the element heights are equal to actual TCFP bearing. Shear deformation occurs at the semi-height of the element. It can be said that the element mass does not affect the result of the analysis. However, it is necessary for efficiency of the analysis.

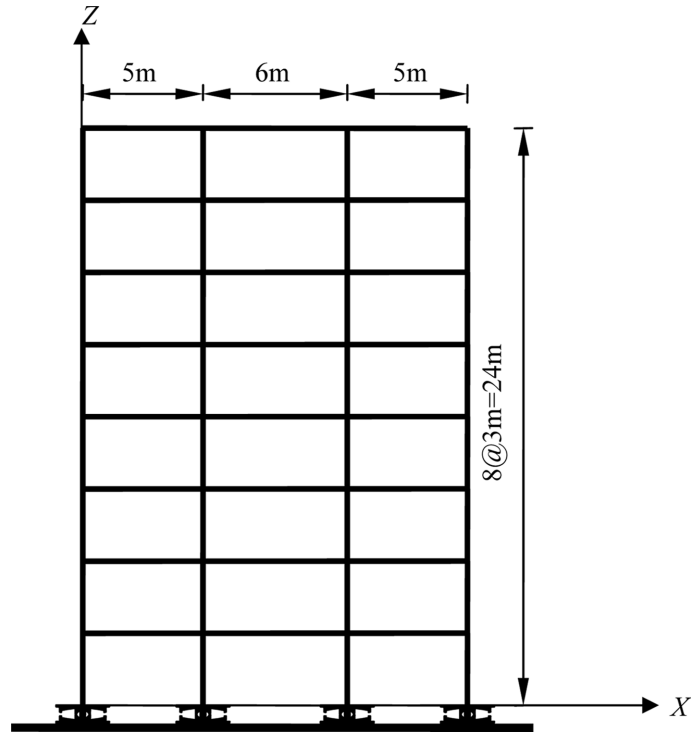


Fig. 5 2D model of the structure

Table 1 Cross-sectional properties of the buildings

Section name	Cross-section (cm/cm)	Inertia moment (m <sup>4</sup> )	Unit volume weight (kN/m <sup>3</sup> )	Modulus of elasticity (MPa)
Columns	30/80 (1 <sup>st</sup> to 2 <sup>nd</sup> stories)	12800		
	30/70 (3 <sup>rd</sup> to 5 <sup>th</sup> stories)	8575	25	28000
	30/50 (6 <sup>th</sup> to 8 <sup>th</sup> stories)	3125		
Beams	30/60	5400	25	28000

Table 2 Actual properties of the TCFP bearings

Name of property	Value
$R_{eff1} = R_{eff4}$ (mm)	1200
$R_{eff2} = R_{eff3}$ (mm)	230
$d_1 = d_4$ (mm)	200
$d_2 = d_3$ (mm)	80
$\mu_1 = \mu_4$	0.040
$\mu_2 = \mu_3$	0.010

Table 3 Parameters of the series model of the TCFP (interior) bearing used in the analysis

FP link element	Friction coefficient $\bar{\mu}_i$	Radii of curvature $\bar{R}_{effi}$ (mm)	Elastic stiffness $K_i$ (kN/m)	Rate parameter $\bar{a}_i$ (sec/mm)	Gap displacement $d_i$ (mm)
FP1 ( $i = 1$ )	0.010	460	8500	0.050	
FP2 ( $i = 2$ )	0.040	970	34000	0.124	162
FP3 ( $i = 3$ )	0.040	970	34000	0.124	162

### 5.1 Properties of the series model for analysis in SAP2000

To properly represent the vertical stiffness of the bearing, the modulus of elasticity of the bearing is specified to be related with that of the steel. The bearing is not exactly a solid piece of metal so that the modulus is reduced to half to approximate the actual situation. So, the modulus of elasticity of the bearings is taken as  $E = 1.05 \times 10^8$  kN/m<sup>2</sup> (Constantinou *et al.* 2007). Hence, the vertical stiffness of the bearing is

$$K_v = \frac{EA}{h} \tag{16}$$

where  $A$  is the area of the slider and  $h$  is the real height of the bearing. Elastic stiffness is, furthermore, equal to

$$K = \frac{\bar{\mu}_i W}{2Y} \tag{17}$$

in which  $\bar{\mu}_i$  is coefficient of friction on the surface  $i$  for high speed motion;  $W$  is axial load supported by the bearing and  $Y$  denotes yield displacement and is taken as 1 mm. Effective stiffness is equal to

$$K_{effi} = \frac{W}{\bar{R}_{effi}} \tag{18}$$

Table 4 Properties of the SCFP link elements used in SAP2000

	SCFP1	SCFP2	SCFP3
Element height (mm)	100	50	100
Shear deformation location (mm)	50	25	50
Supported weight (kN)	1700	1700	1700
Vertical stiffness (kN/m)	4174882	4174882	4174882
Elastic stiffness (kN/m)	8500	34000	34000
Effective stiffness (kN/m)	3696	1753	1753
Friction coefficient-fast	0.010	0.040	0.040
Friction coefficient-slow	0.005	0.020	0.020
Radius (mm)	460	970	970
Rate parameter (sec/mm)	0.050	0.124	0.124

where  $\bar{R}_{effi}$  is  $i$ th element of the effective radius. Besides, rate parameter is coefficient dependent velocities which provide transition between maximum and minimum value of coefficient of friction, and is taken as to be 0,1 sec/mm for each actual sliding surfaces 1 to 4. By means of Eqs. (16) to (18), the properties of the SCFP link element utilized in SAP2000 (2007) is summarized in Table 4. Herein the friction coefficient-slow stands for the half of the friction coefficient at the high speed motion.

Unidirectional excitation along the  $X$ -axis of the building is applied using the GBZ000 component of the 1999 Kocaeli earthquake recorded at Gebze station in Fig. 6, the TCU129-W component of the 1999 Chi-Chi earthquake recorded at TCU129 station in Fig. 7, and the ELC-270 component of the 1940 Imperial Valley earthquake recorded at 117 El-Centro Array #9 station in Fig. 8, separately. The peak acceleration and displacement of the ground motions are 0.244 g and 424.70 mm for the Kocaeli earthquake, 1.01 g and 501.50 mm for the Chi-Chi earthquake, and 0.215 g and 239.10 mm for the Imperial Valley earthquake, respectively. The motions are scaled by a factor of 2 in order to show all possible sliding positions of the TCFP bearing. The TCFP bearing is modeled using the SCFP and the gap link elements having nonlinear properties. Time history analysis is carried out for the isolated and non-isolated buildings. The first five periods of vibration of the isolated with different type friction pendulum bearings and the non-isolated buildings obtained from the analysis are given in Table 5. Acceleration and displacement response values of the isolated building using the SCFP, the DCFP and the TCFP bearings are compared in Table 6 when the building is subjected to the Kocaeli earthquake.

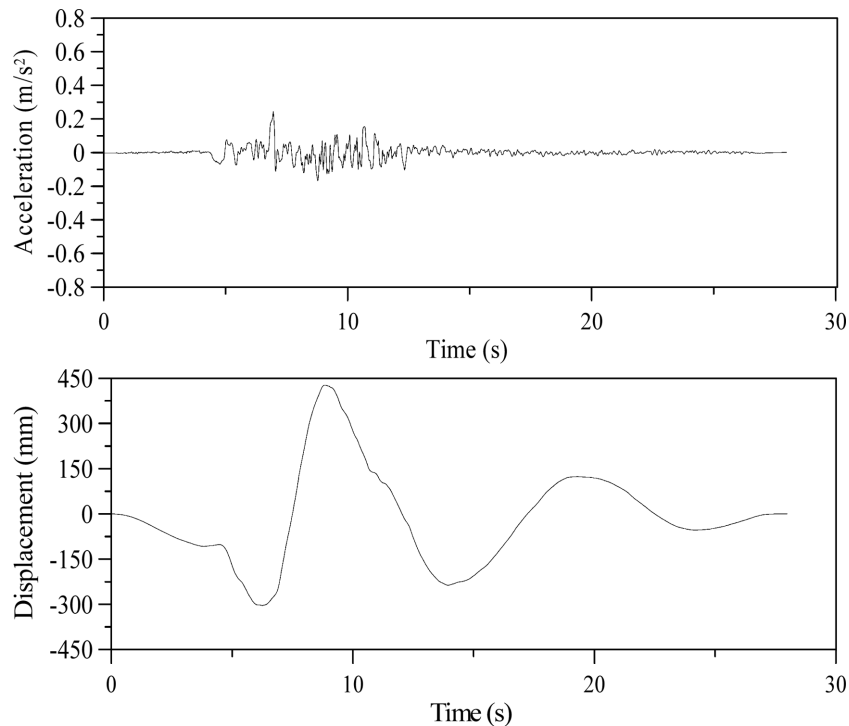


Fig. 6 Acceleration and displacement histories of the 1999 Kocaeli earthquake recorded at Gebze station

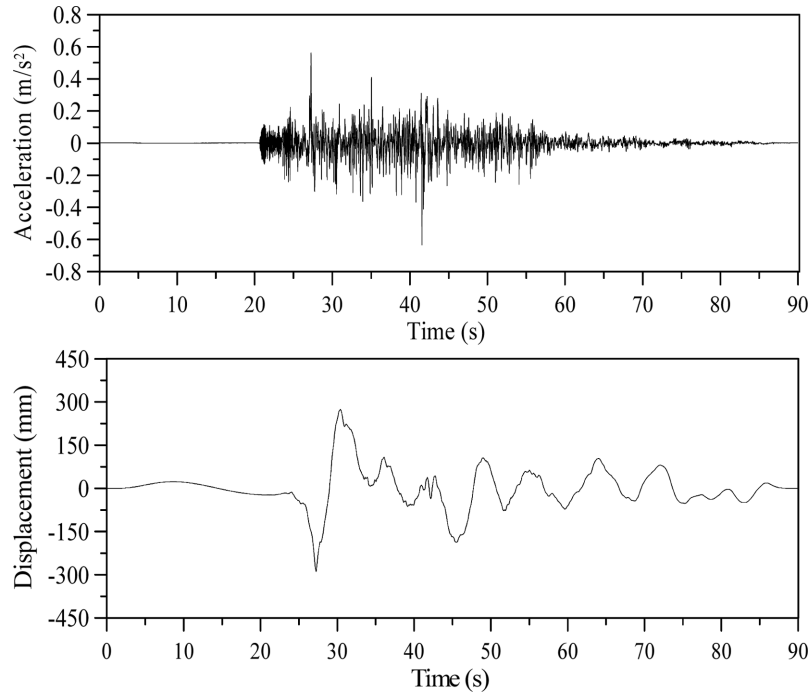


Fig. 7 Acceleration and displacement histories of the 1999 Chichi earthquake recorded at TCU129 station

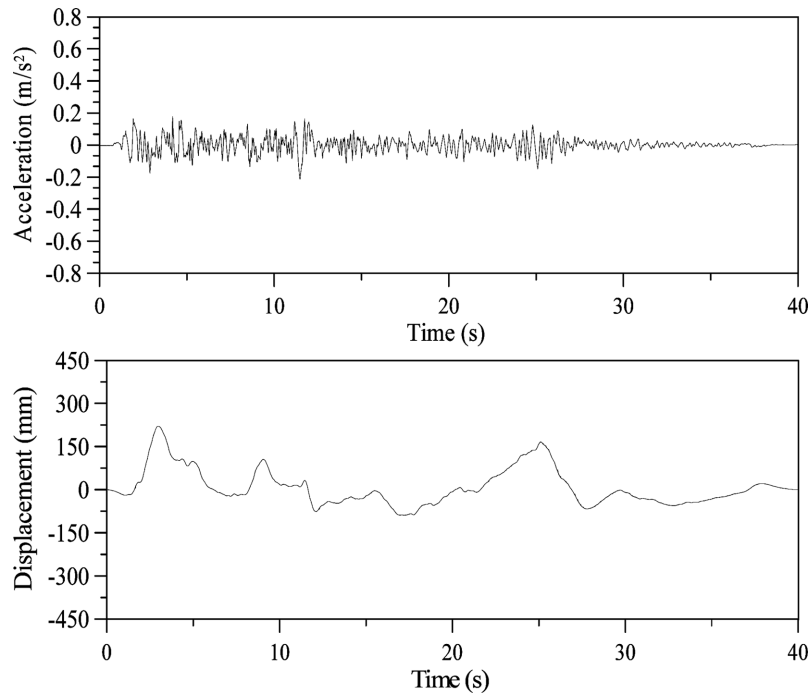


Fig. 8 Acceleration and displacement histories of the 1940 Imperial Valley earthquake recorded at 117 El Centro Array #9 station

Table 5 Periods for the isolated buildings for friction pendulums and non-isolated buildings

Mode Number	Period (sec)			
	Isolated Building			Non-Isolated Building
	with SCFP	with DCFP	with TCFP	
1	2.286	2.986	3.219	0.885
2	0.464	0.473	0.482	0.306
3	0.224	0.225	0.228	0.169
4	0.140	0.141	0.159	0.119
5	0.112	0.112	0.158	0.106

Table 6 Comprising of friction pendulum bearing types

Level	SCFP		DCFP		TCFP	
	Acceleration (m/sn <sup>2</sup> )	Displacement (mm)	Acceleration (m/sn <sup>2</sup> )	Displacement (mm)	Acceleration (m/sn <sup>2</sup> )	Displacement (mm)
1. floor	4.406	106.30	3.715	139.50	3.713	416.10
2. floor	4.824	117.30	3.696	146.80	3.719	424.90
3. floor	4.374	129.80	4.158	154.60	3.771	434.10
4. floor	4.293	141.60	4.139	161.90	3.670	441.90
5. floor	4.228	152.20	3.870	168.50	3.638	448.30
6. floor	4.949	163.80	4.360	175.40	3.812	454.60
7. floor	5.757	172.30	4.378	180.40	3.920	458.80
8. floor	6.099	177.40	4.356	183.30	4.091	461.20

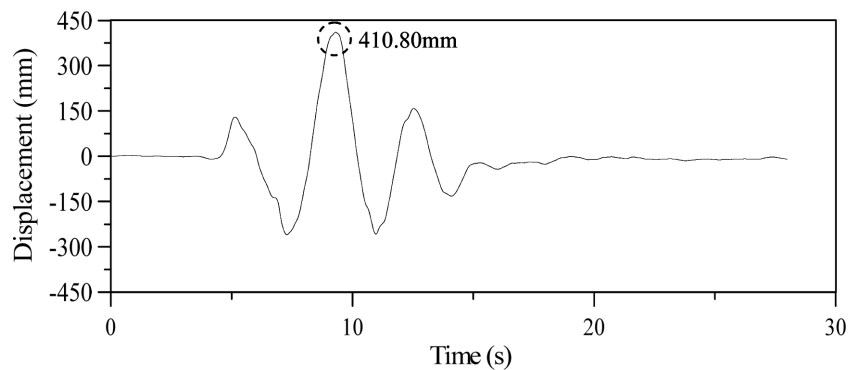


Fig. 9 Displacement history of the TCFP bearing for the Kocaeli earthquake

The displacements of the TCFP bearings obtained from analyses are depicted in Figs. 9-11. It is seen from the figures that maximum displacement reaches to 410.80 mm, 290.10 mm and 291.40 mm in case of the Kocaeli, the Chi-Chi and The Imperial Valley earthquakes, respectively. Displacement capacity of the TCFP bearings is intended as 413.80 mm. The peak displacement of the ground motions as mentioned above are 424.70 mm, 501.50 mm and 239.10 mm for the

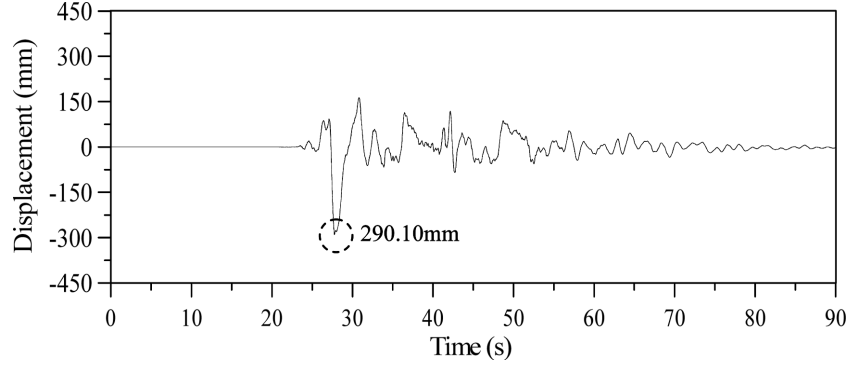


Fig. 10 Displacement history of the TCFP bearing for the Chi-Chi earthquake

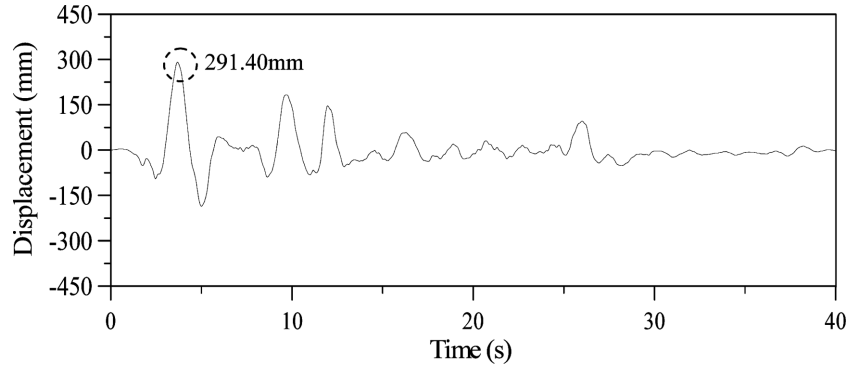


Fig. 11 Displacement history of the TCFP bearing for the Imperial Valley earthquake

Kocaeli, Chi-Chi and Imperial Valley earthquakes, respectively. These values show that the motion firstly starts inner surfaces 2 and 3 only. At the position of the bearing uses own approximately 13.80 mm displacement capacity given by Eqs. (19) and (20) when the forces acting on the surfaces 2 and 3 are up to value of 68 kN calculated by the Eqs. (23) and (24). Then the motion stops on surface 2 and sliding occurs on surfaces 1 and 3 as long as friction forces are to be between 68 kN and 351.33 kN calculated by the Eqs. (25) and (26); this time the bearing may approach totally 410.80 mm-displacement capacity given by Eq. (21). Afterwards the friction forces exceed to 351.33 kN, the displacement of the TCFP bearing goes to maximum values of 410.80 mm when the building is subjected to the Kocaeli earthquake as shown is Fig. 9.

$$u_I = (\mu_1 - \mu_2)R_{eff\ 2} + (\mu_1 - \mu_3)R_{eff\ 3} \quad (19)$$

$$u_{II} = u_I + (\mu_4 - \mu_1)(R_{eff\ 1} + R_{eff\ 3}) \quad (20)$$

$$u_{III} = u_{II} + \left(1 + \frac{R_{eff\ 4}}{R_{eff\ 1}}\right)d_1 - (\mu_4 - \mu_1)(R_{eff\ 1} + R_{eff\ 4}) \quad (21)$$

$$u_{IV} = u_{III} + \left[\left(\frac{d_4}{R_{eff\ 4}} + \mu_4\right) - \left(\frac{d_1}{R_{eff\ 1}} + \mu_1\right)\right](R_{eff\ 2} + R_{eff\ 4}) \quad (22)$$

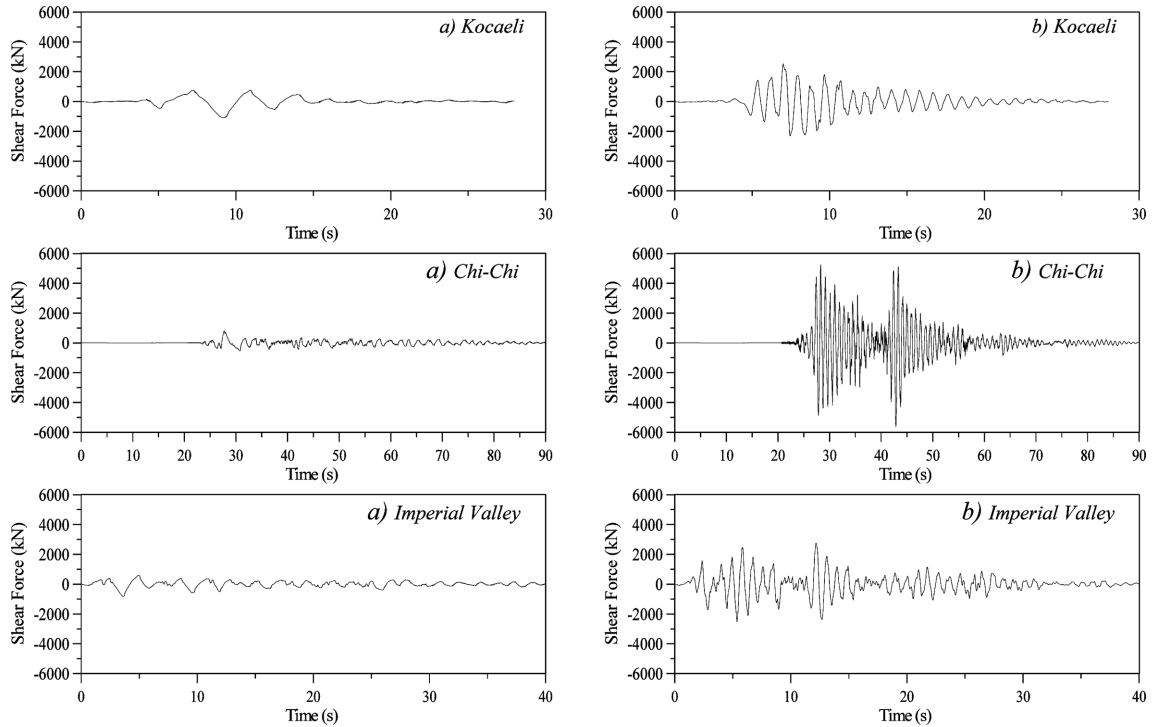


Fig. 12 Base shear force histories of (a) the isolated and (b) the non-isolated buildings

where  $u_I$ ,  $u_{II}$ ,  $u_{III}$  and  $u_{IV}$  are the displacements occurring on the surfaces at the different possible positions of the motion. The other parameters are defined beforehand. Base shear forces for the isolated and non-isolated building are also plotted in Fig. 12. The base shear force at the bearing level is approximately obtained as  $0.646 W$ ,  $0.480 W$  and  $0.493 W$  for the Kocaeli, the Chi-Chi and the Imperial Valley earthquakes, respectively. Moreover, the base shear force of the non-isolated building is  $1.498 W$ ,  $3.308 W$  and  $1.631 W$  for the Kocaeli, the Chi-Chi and the Imperial Valley earthquakes, respectively. The results show that the TCFP bearings significantly reduce the base shear forces. The decrement values are ranging from 57% to 85% in case of the usage of the three earthquake records.

Figs. 13-15 give an opportunity to compare the structural accelerations at the first, fourth and top floor levels during the three earthquakes. It is seen from these figures, accelerations transmitted to the building decrease by means of using the isolation technique when the accelerations increase throughout the floor levels of the non-isolated building.

Similarly, the first, fourth and top floor displacement histories of the considered building are presented in Figs. 16-18, respectively. These figures demonstrate that relative displacement at the each floor is approximately zero at the isolated building with the TCFP bearings. On the other hand, the floor displacements of the non-isolated building increase throughout the first to top floor levels. The maximum displacements obtained from the time history analysis of the building subjected to the Kocaeli earthquake are approximately 461.23 mm and 179.37 mm for the isolated and non-isolated buildings, respectively. The displacement at the TCFP bearing level is considered as 410.80 mm, the maximum top displacement for the isolated building is turned out to be as 50.43 mm.

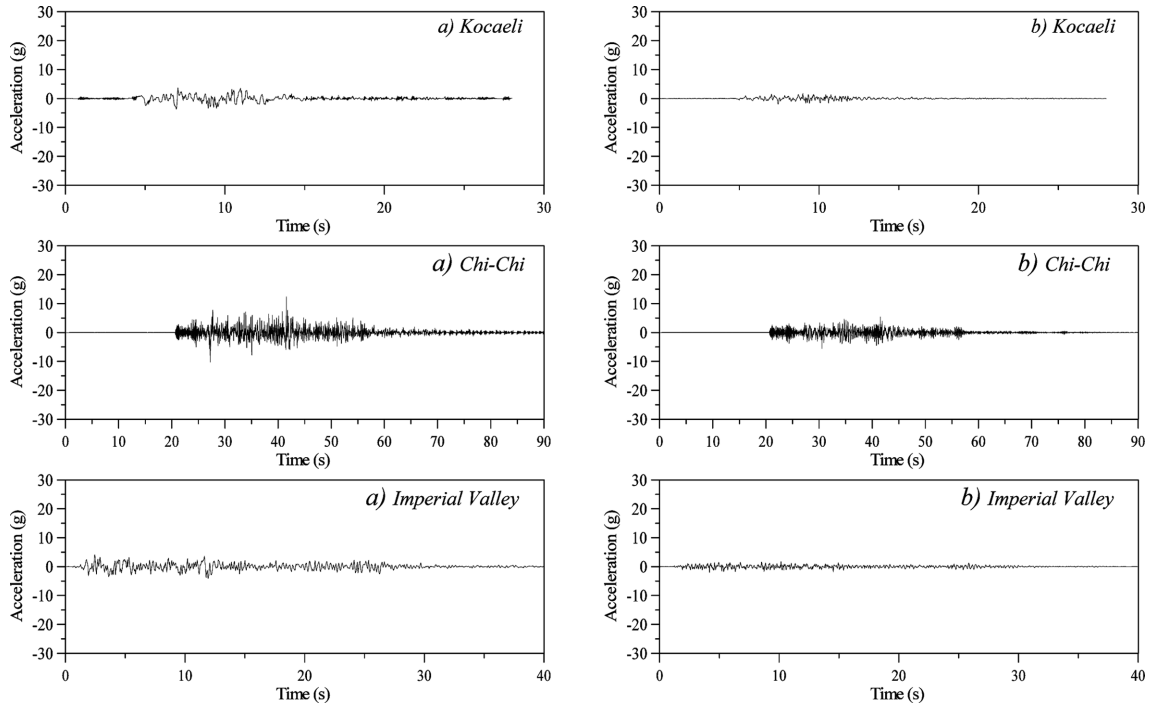


Fig. 13 First floor acceleration histories of (a) the isolated and (b) the non-isolated buildings

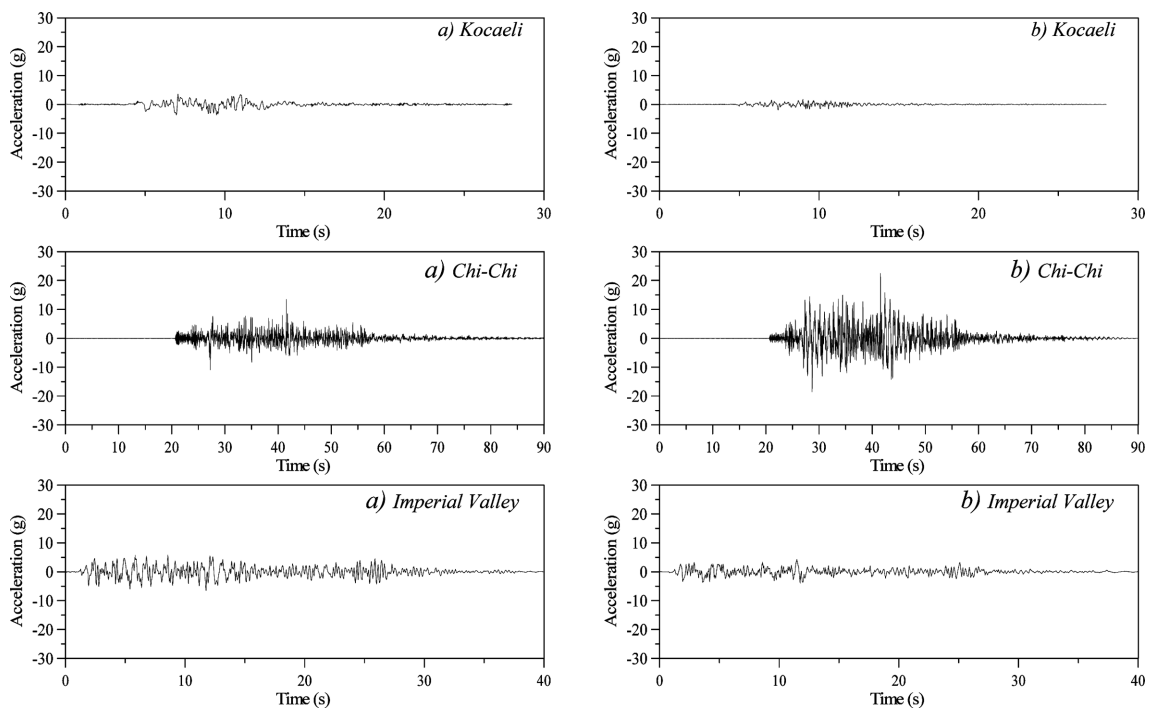


Fig. 14 Fourth floor acceleration histories of (a) the isolated and (b) the non-isolated buildings

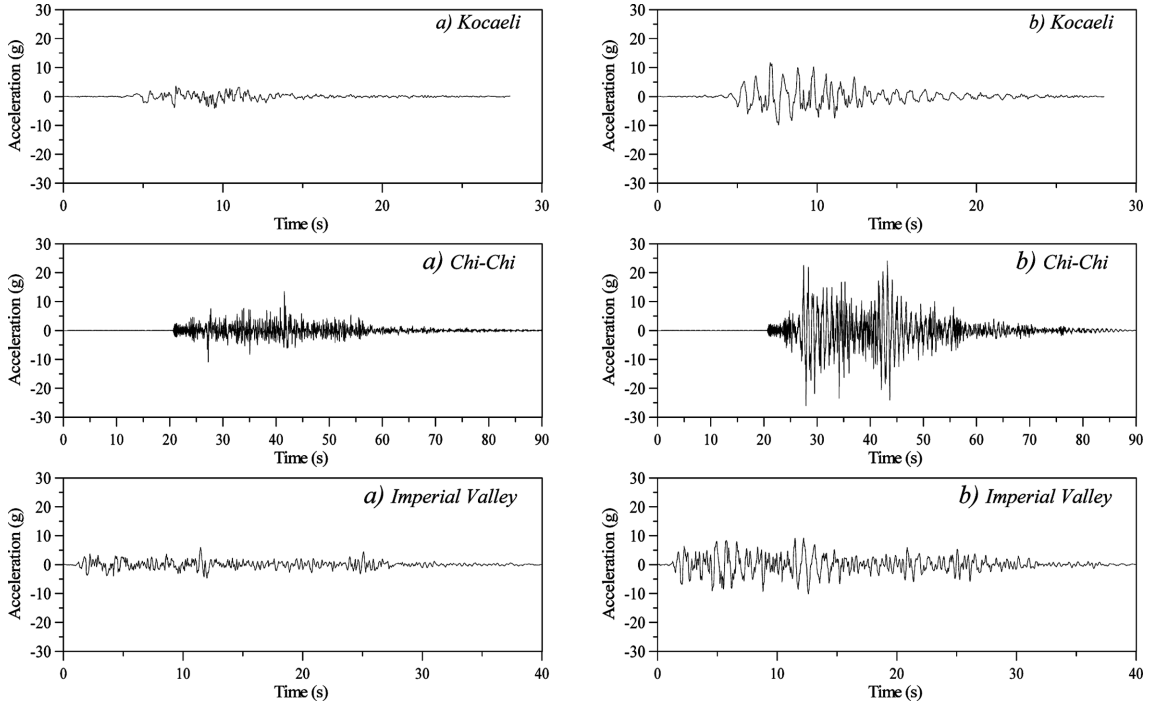


Fig. 15 Top floor acceleration histories of (a) the isolated and (b) the non-isolated buildings

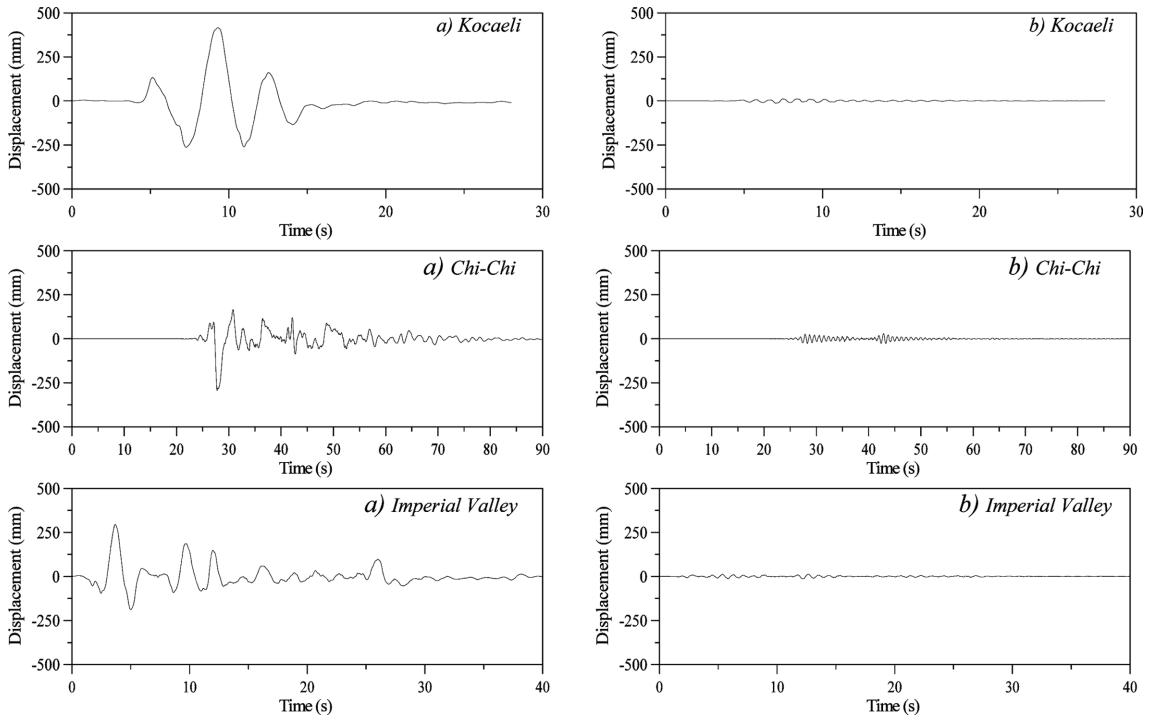


Fig. 16 First floor total displacement histories of (a) the isolated and (b) the non-isolated buildings

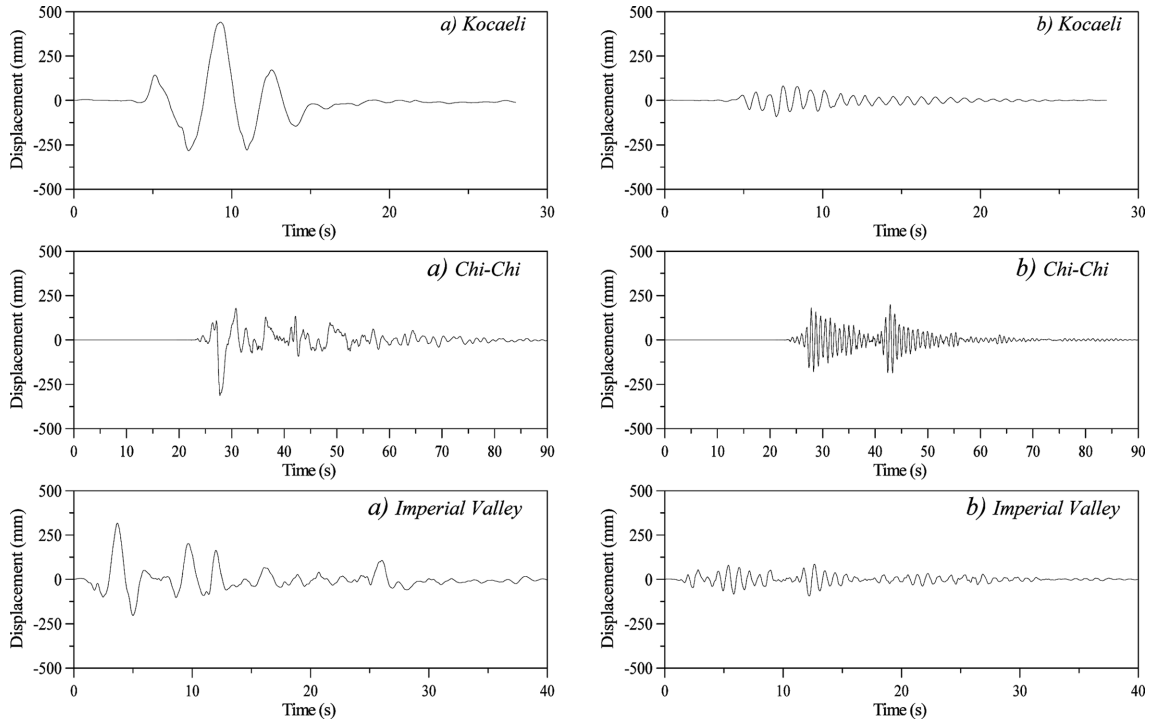


Fig. 17 Fourth floor total displacement histories of (a) the isolated and (b) the non-isolated buildings

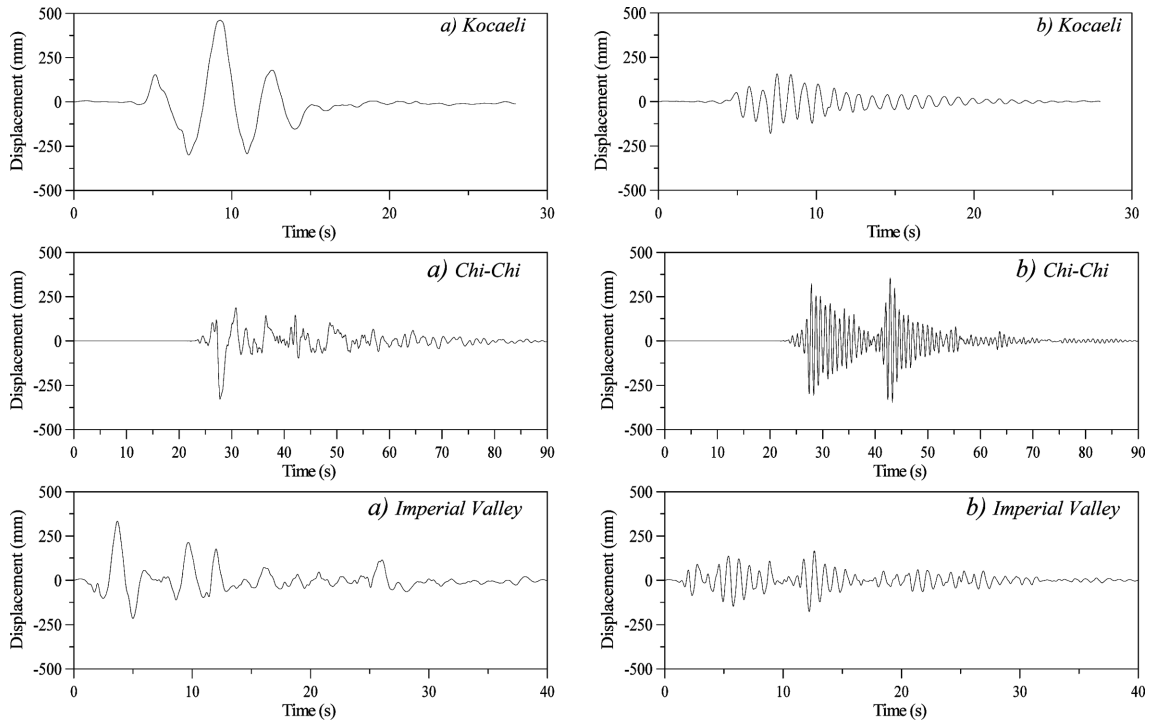


Fig. 18 Top floor total displacement histories of (a) the isolated and (b) the non-isolated buildings

The maximum displacements obtained from the time history analysis of the building subjected to the Chi-Chi earthquake are approximately 329.09 mm and 356.15 mm for the isolated and non-isolated buildings, respectively. The displacement at the TCFP bearing level is considered as 290.10 mm, the maximum top displacement for the isolated building is remaining 38.99 mm.

The maximum displacements obtained from the time history analysis of the building subjected to the Imperial Valley earthquake are approximately 334.34 mm and 176.17 mm for the isolated and non-isolated buildings, respectively. The displacement at the TCFP bearing level is considered as 291.40 mm, the maximum top displacement for the isolated building became 42.94 mm.

Displacements between the floors of the isolated building are smaller than those of the non-isolated building. Hence, inertia forces such as bending moment, axial and shear forces decrease. The decrements at the floor level of the isolated building in accordance with the non-isolated building are between 72% and 89%.

$$F_I = \mu_1 W \quad (23)$$

$$F_{II} = \mu_4 W \quad (24)$$

$$F_{III} = \frac{W}{R_{eff1}} d_1 + \mu_1 W \quad (25)$$

$$F_{IV} = \frac{W}{R_{eff4}} d_4 + \mu_4 W \quad (26)$$

where  $F_I$ ,  $F_{II}$ ,  $F_{III}$  and  $F_{IV}$  are the shear forces occurring on the surfaces at the different possible positions of the motion.

## 6. Conclusions

A two dimensional- and eight- story of a building with and without isolation system is compared in this study. The building isolated by the TCFP bearing is subjected to three different ground motions. Time history analysis in order to investigate of the effectiveness of the seismic isolation systems on the buildings is performed. Additionally the TCFP bearing is to be modeled as of a series arrangement of the three SCFP bearings. The ground motion of the Kocaeli earthquake is used to compare isolated buildings with different friction type isolation bearings, that is, the SCFP, the DCFP and the TCFP bearing system.

Analyses are performed for the isolated and non-isolated building subjected to different ground motions. And then results obtained from time history analysis were compared. The study demonstrated that relative displacement at the floor is approximately zero at isolated building with the TCFP bearing subjected to different ground motions. The relative structural displacements as expected are increased when comparing with these of non-isolated building. This is because of the demand displacement capacity of the TCFP bearings. Provide that the displacement capacity at the TCFP bearing level is considered, it is seen that displacement for the isolated building is smaller than these of non-isolated building. In the TCFP bearing, peak accelerations at floor level are smaller than SCFP and DCFP. To the contrary displacement capacity of the TCFP is bigger than the other.

Accelerations transmitted to the building reduce by means of using the isolation technique. Usage of the TCFP bearings to isolate structures against severe earthquakes provides more major benefits than the SCFP and DCFP in order to protect the structures and then living in them.

Finally, it should be noted that isolation system such as the TCFP bearing is effective when the structures are subjected to severe earthquakes. In this study, the results are obtained for three different earthquake records.

## References

- Computers and Structures Inc. (2007), SAP2000: Static and Dynamic Finite Element Analysis of Structures, Berkeley, CA, USA.
- Fabio, F. and Constantinou, M.C. (2010), "Evaluation of simplified methods of analysis for structures with triple friction pendulum isolators", *Earthq. Eng. Struct. D.*, **39**, 5-22.
- Fenz, D.M. and Constantinou, M.C. (2008b), "Spherical sliding isolation bearings with adaptive behavior: theory", *Earthq. Eng. Struct. D.*, **37**, 163-183.
- Fenz, D.M. and Constantinou, M.C. (2008c), "Modeling triple friction pendulum bearings for response history analysis", *Earthq. Spectra*, **24**, 1011-1028.
- Fenz, D.M. and Constantinou, M.C. (2008d), "Spherical sliding isolation bearings with adaptive behavior: experimental verification", *Earthq. Eng. Struct. D.*, **37**, 185-205.
- Fenz, D.M. and Constantinou, M.C. (2008a), "Development, implementation and verification of dynamic analysis models for multi-spherical sliding bearings", Technical Report MCEER-08-0018, Multidisciplinary Center for Earthquake Engineering Research, University at Buffalo, State University of New York, Buffalo, NY.
- Fenz, D.M. and Constantinou, M.C. (2006), "Behaviour of the double concave friction pendulum bearing", *Earthq. Eng. Struct. D.*, **35**, 1403-1424.
- Kelly, J.M. (1999), "The role of damping in seismic isolation", *Earthq. Eng. Struct. D.*, **28**(1), 3-20.
- Khoshnoudian, F. and Rabiei, M. (2010), "Seismic response of double concave friction pendulum base-isolated structures considering vertical component of earthquake", *Adv. Struct. Eng.*, **13**(1), 1-14.
- Kim, Y.S. and Yun, C.B. (2007), "Seismic response characteristics of bridges using double concave friction pendulum bearings with tri-linear behavior", *Eng. Struct.*, **29**, 3082-3093.
- Lin, B.C. and Tadjbakhsh, I.G. (1986), "Effect of vertical motion on friction driven systems", *Earthq. Eng. Struct. D.*, **14**, 609-622.
- Morgan, T.A. and Mahin, S.A. (2008), "Performance-based design of seismic isolated buildings considering multiple performance objectives", *Smart Struct. Syst.*, **4**(5), 655-666.
- Mostaghel, N. and Tanbakuchi, J. (1983), "Response of sliding structures to earthquake support motion", *Earthq. Eng. Struct. D.*, **11**, 729-748.
- Panchal, V.R., Jangid, R.S., Soni, D.P. and Mistry, B.B. (2010), "Response of the double variable frequency pendulum isolator under triaxial ground excitations", *J. Earthq. Eng.*, **14**, 527-558.
- Soni, D.P., Mistry, B.B. and Panchal, V.R. (2010), "Behaviour of asymmetric building with double variable frequency pendulum isolator", *Struct. Eng.*, **34**(1), 61-84.
- Tsai, C.S. and Lin, Y.C. (2009), "Mechanical Characteristics and Modeling of Multiple Trench Friction Pendulum System with Multi-intermediate Sliding Plates", *World Academy of Science, Engineering and Technology J: Mechanical and Aerospace Engineering*, **4**(1), 39-51.
- Tsai, C.S., Chen, W.S. and Chiang, T.C. (2010), "Experimental and numerical studies of trench friction Pendulum system", *Struct. Eng. Mech.*, **34**(2), 277-280.
- Tsai, C.S., Chiang, T.C. and Chen, B.J. (2003), "Finite element formulations and theoretical study for variable curvature friction pendulum system", *Eng. Struct.*, **25**, 1719-1730.
- Zayas, V.A., Low, S.S. and Mahin, S.A. (1990), "A simple pendulum technique for achieving seismic isolation", *Earthq. Spectra*, **6**, 317-334.

Zekioglu, A., Darama, H. and Erkus, B. (2009), "Performance-based seismic design of a large seismically isolated structure: istanbul sabiha gokcen international airport terminal building", *Structural Engineering Association of California Convention Proceedings*, 409-427.